IEEE Access
Multidisciplinary | Rapid Review | Open Access Journal

Received November 18, 2019, accepted December 29, 2019, date of publication January 6, 2020, date of current version January 27, 2020.

Digital Object Identifier 10.1109/ACCESS.2020.2964001

Direction-Decision Learning Based Pedestrian Flow Behavior Investigation

ZHE ZHANG AND LIMIN JIA

State Key Laboratory of Rail Traffic Control and Safety, Beijing Jiaotong University, Beijing 100044, China

Corresponding author: Limin Jia (lmjia@bjtu.edu.cn)

This work was supported in part by the National Natural Science Foundation of China under Grant 71801009, in part by the National Key Research and development Program of China under Grant 2018YFB1201403, and in part by the Fundamental Research Funds for the Central Universities under Grant 2019RC037.

ABSTRACT To investigate the pedestrian flow behavior in corridors, a microscopic simulation model of pedestrian flow is proposed in this paper based on the desired-direction-decision learning and social force model. The proposed model is composed of two parts: direction-decision and walking behavior decision. First, the decision tree model is proposed to predict the walking direction of pedestrians by comparing the prediction and simulation performance of three different models. Then, to avoid collisions between pedestrians and obstacles, the acceleration model and the collision avoidance model are proposed to compute the walking speed. Finally, an computational experiment is conducted to simulate crowd movement in corridors. The experimental results show that the proposed model can suggest the shortest overtaking route for individual pedestrians among four models, and the speed-density relationship fits the experimental data well. The sensitive analysis shows that the lanes in bidirectional pedestrian flow can be formed much more easily if the pedestrians have higher direction changing frequency, and there is an optimal visibility field (2.8) to realize the highest traffic efficiency.

INDEX TERMS Pedestrian flow, simulation, direction decision learning, decision tree.

I. INTRODUCTION

The mathematical modeling of pedestrian flow has gained much scientific interest in recent decades because pedestrian movement is an important component in both fields of safety and capacity assessment of walking facilities [1], [2]. Previous studies have focused on investigating the characteristics of pedestrian flow by simulation. Several microscopic models have been proposed in the past to provide a more detailed description of individual behavior and interactions. Generally, the existing microscopic models can be categorized as discrete and continuum models [3].

The most popular discrete models used in recent research include the lattice gas model (LGM) [4], [5] and the cellular automata model (CAM) [6]–[9], in which the space is discretized to approximate real pedestrian movement. The evolution of the pedestrians in time is determined by physical and social laws that describe the interaction among the particles as well as their interactions with the physical surroundings. Collision avoidance can be realized by defining mandatory movement rules in these models [10]. The floor field is defined in CAM to lead the pedestrians to the targets, and game theory is employed to solve the competition behavior of pedestrians in LGM [11]. Compared to the continuum models, the discrete models can be computed efficiently. However, the discrete models have low capability to address various walking speeds because the update scheme depends on the walking speed of pedestrians. For example, only three values of walking speed are considered in CAM [12], and four update schemes are introduced into CAM [13]. In addition to the limitation of walking speed, the number of walking directions of pedestrians in discrete models is also limited. For example, at most 8 direction choices exist when the walking space is discretized into square cells, while the number is 6 when the walking space is discretized into hexagonal cells [14]. Therefore, it is difficult to describe the variety of pedestrian movement directions and speeds using discrete models.

Because of the limitation of discrete models, continuum models have been developed. The typical models include the social force model (SFM) and velocity models (VM). However, the VM is not suitable for simulation of crowd movement because it does not consider the interaction between pedestrians [15], [16] except [17]. Therefore, the most

The associate editor coordinating the review of this manuscript and approving it for publication was Sabah Mohammed.

popular continuum model is the SFM. The SFM was proposed by Helbing [18] to simulate crowd evacuation and self-organization, and then the extended or modified SFM was developed by considering many more real-life factors [19]. These extensions can be found in [20]. However, if repulsive forces from other pedestrians exceed the acceptable level, the pedestrian may move backward, which is unrealistic [21]. Moreover, many parameters of SFM need to be calibrated based on video data [22]–[24].

In fact, the pedestrian can choose the walking direction or route based on the neighboring environment, and thus, the desired direction should be updated in the pedestrian flow simulation model. The route choice model has been developed based on the utility theory [25], [26]. However, it may not be suitable for pedestrian traffic because the direction choice of pedestrians is approximately continuous. A linear model was also proposed to determine the walking direction of pedestrians in real time [27]; however, the movement rules in the proposed method did not consider collision avoidance to improve simulation efficiency. Similarly, the heuristic method was also proposed to compute the desired walking direction, which was a trade-off between avoiding obstacles and minimizing detours from the most direct route [28], [29]. With the development of artificial intelligence, the machine learning method has been used to simulate pedestrian flow due to the development of pedestrian detection [9]. For example, a multiagent reinforcement learning-based framework was proposed to simulate pedestrian groups [30], and a data-driven neural network approach and an artificial intelligence-based approach were proposed to simulate the pedestrian flow [16], [31]. The social long short-term memory model was also proposed to predict the pedestrian trajectory [32], [33]. They used the trajectory data to train the neural network model, and the trained model produced the real-time velocity in the simulation environment. However, the conflicts between pedestrians cannot be avoided if the predicted velocity is not sufficiently accurate, and the model performance relies much on the prediction performance.

To overcome this shortcoming, we proposed a new simulation model of pedestrian flow by combining the advantages of the artificial intelligence method and SFM in this paper. Within this approach, the desired direction is produced by the prediction model. The prediction models are trained using real-life data, and the best model is selected based on the prediction and simulation performance. First, the desired direction model learns the complex relationship between the direction decision and the neighboring environment, which can be represented by a number of features. The psychological behavior of pedestrians can be simulated. Second, the proposed model is calibrated by a large quantity of trajectory data, and thus, can be incorporated into other simulation models. Finally, the social force model is used to solve the collision problem, which may not be solved by only the machine learning method.

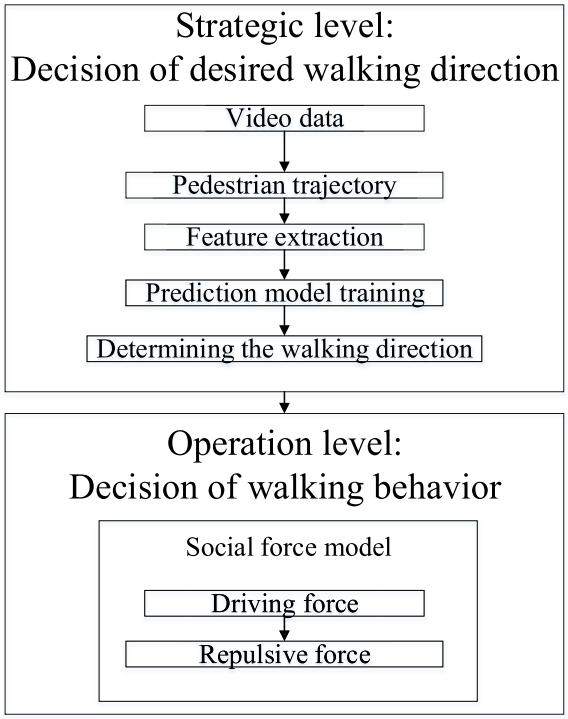

FIGURE 1. General structure of the model.

II. MODEL FRAMEWORK

As shown in Fig.1, the general structure of the model is based on the decision-making level of the psychological process. The first level is the strategic level, at which pedestrians make a decision of the intended direction. The second level is the operational level, which is the second step for pedestrians to adjust their walking behavior in the corridors. Pedestrians adjust their speeds and directions dynamically when interacting with other pedestrians and obstacles.

III. DIRECTION DECISION MODEL

A. FEATURE SELECTION

The desired direction of pedestrians is affected by the local environment and their destination. The desired direction of pedestrians is affected by the pedestrians and obstacles in his/her visual field because the pedestrians try to keep distance from each other and avoid potential collision with others in the walking direction. Each pedestrian desires to arrive at his/her destination and thus the desired direction is also determined by the location of destination. Therefore, the relative distance and speed are selected as features to predict the desired direction. The pedestrians flow in bidirectional corridors as shown in Fig.2 will be investigated in this paper and the distance features influencing the desired walking direction can be calculated as follows:

$$D = [x_i - x_j, y_i - y_j, \frac{y_i}{W}, \frac{L - x_i}{L}] \tag{1}$$

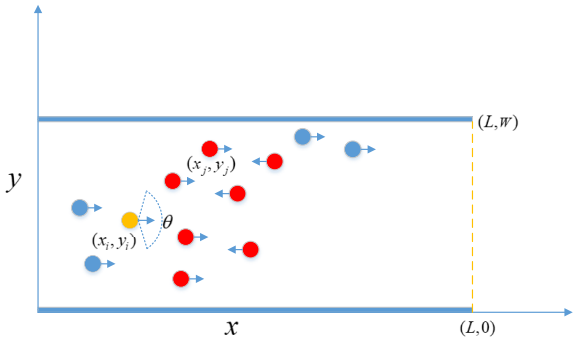

FIGURE 2. Feature selection.

in which (x_i, y_i) and (x_j, y_j) are the coordinates of pedestrians, and L and W denote the length and width of the corridor. $x_i - x_j$, $y_i - y_j$ denote the relative horizontal distance and vertical distance between pedestrians i and neighboring pedestrian j. $\frac{L-x_i}{L}$ denotes the distance to the end point of corridor and $\frac{y_i}{W}$ denotes the distance to the wall. In order to reduce the number of used features, the distance between pedestrian i and walls is normalized so that the distance to only one wall can represent the relative position to the two walls. Further, the trained model can be used to predict the desired direction of pedestrians in corridors with various lengths and widths due to the normalized distance.

Pedestrian does not change his/her current walking direction abruptly and frequently and the current movement direction can be represented by the horizontal and vertical speed. The relative speed between pedestrians also affects the direction decision of pedestrians [34] because the relative speed represents the change rate of relative distance. Therefore, the speed features influencing the desired walking direction can be formulated as follows:

$$V = [v_i^x, v_i^y, v_i^x - v_j^x, v_i^y - v_j^y] \tag{2}$$

where v_i^x *and* v_i^y are the horizontal and vertical speeds of pedestrian i. $v_i^x - v_j^x$ *and* $v_i^y - v_j^y$ denote the relative horizontal and vertical speed. As shown in Fig.2, there are 9 pedestrians in the visibility field of the yellow pedestrian; however, only 7 pedestrians are selected to produce the features to efficiently predict the walking direction in this paper because more features reduce the computing efficiency. Finally, 32 features are selected to train the prediction model. Let β denote the set of features. The relative distance and speed features are listed in ascending order of distance. Based on the trajectory data, we can obtain the position vector $\overrightarrow{\eta}$ from the position at time t to the position at time $t + \Delta t$. The desired walking direction α is represented by the angle between $\overrightarrow{\eta}$ and the vector $\overrightarrow{\upsilon} = [0, -1]$. Therefore, α can be formulated as follows:

$$\alpha = \arccos\left(\frac{\overrightarrow{\eta}\,\overrightarrow{\upsilon}}{\|\overrightarrow{\eta}\|}\right) \tag{3}$$

Finally, we obtain the output and input of the direction decision model and the relationship between the desired walking direction and features can be built and examined.

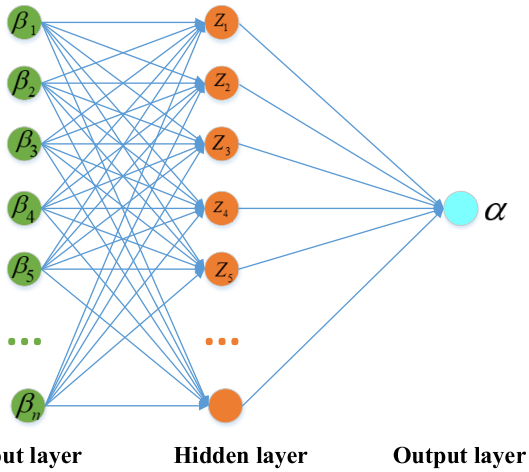

FIGURE 3. The common structure of the neural network model.

B. MODEL SELECTION

There are many popular models, such as regression models, neural network models and decision tree models, that build the link between the walking direction and features [35]. To select the best prediction model. The performance evaluation method is proposed in this section. The model selection method is inspired by [36]; however, we introduce more indicators to measure the model performance.

1) LINEAR REGRESSION (LR) MODEL

Regression analysis is one of the most popular techniques for predictive modeling because it assumes that there is a linear relationship between outputs and inputs. A multiple regression model with more than one input feature can be formulated as follows:

$$\alpha = A\beta^T + B \tag{4}$$

where A and B are the regression parameters. The least-squares method is generally used for estimating the parameters in the regression model. Once the regression parameters are obtained, a prediction equation can then be used to predict the walking direction as a linear function of distance and speed features.

2) NEURAL NETWORK (NN) MODEL

The neural network model is also a popular prediction model when the prior knowledge on the relationship between the output variables and input features is unknown; it was originally developed by researchers attempting to mimic the neurophysiology of the human brain. The common structure of the neural network model is depicted in Fig.3. The neural network consists of three layers: input layer, hidden layers and output layer. In our model, one hidden layer network is adequate. Each layer has a number of neurons. The numbers of neurons in the input layer (N_{in}) and output layer (N_{out}) are determined by the number of input features and output variables, which are equal to 32 and 1 in our application, respectively. Because too many hidden neurons reduce the

training efficiency, and too few hidden neurons may result in low prediction accuracy, many approaches have been proposed to determine the number of hidden neurons. The method proposed by Ward System [37] is used to set the number of hidden neurons N_h, that is:

$$N_h = \frac{N_{in} + N_{out}}{2} + \sqrt{N_s} \tag{5}$$

where N_s is the number of training samples.

The feed-forward neural network is applied in this paper. The input layer performs the following computation of the inputs, the inputs $\beta_1, \beta_2, ...\beta_n$ are multiplied by the weight before it reaches the node. Once the weighted signals are collected at the node, these values are added to be the weighted sum. The equation of the weighted sum can be written with matrices as

$$V_h = \omega_h \beta + b_h \tag{6}$$

Where V_h, ω_h and b_h denote the activation, weight and bias, respectively. The node enters the weighted sum into the activation function and yields its output. The activation function determines the behavior of the node.

$$Z = \varphi(V_h) \tag{7}$$

$\varphi(\cdot)$ of this equation is the activation function. The most used activation function is the sigmoid [38]. Similar with the input layer, the hidden units are combined to give the activations V_o of the output layer:

$$V_o = \omega_o Z + b_o \tag{8}$$

Finally, the activation function H is applied to obtain the output, which, in this case, is the value of walking direction α

$$\alpha = H(V_o) \tag{9}$$

Given the inputs β and the output α, the proposed neural network model can be trained to minimize the loss function in supervised way [38].

3) DECISION TREE (DT) MODEL

The decision tree model is also a popular prediction method because a series of simple rules is usually developed to divide the outputs into a number of segments. The walking direction can be predicted by the repetitive process of splitting. The most common tree methods include chi squared automatic interaction detection (CHAID), classification and regression trees (CART), and C4.5 and C5.0 [39]. The CART is used to create the decision tree, and the least squared method is used to produce the decision tree [40]. For each feature, the splitting node can be obtained by solving the problem:

$$\min_{l,s}(\min_{c_1} \sum_{\beta_k \in R_1(l,s)} (\alpha_k - c_1)^2 + \min_{c_2} \sum_{\beta_k \in R_2(l,s)} (\alpha_k - c_2)^2) \tag{10}$$

where l denotes the splitting feature and s denotes the value of splitting the node. β_k denotes the kth feature. c_1 and c_2 are the average values of the desired walking direction belonging to the two areas. $R_1(l, s)$ and $R_2(l, s)$ denote the two areas divided by the splitting node:

$$R_1(l, s) = \{\beta | \beta_k \leq s\}, R_2(l, s) = \{\beta | \beta_k > s\} \tag{11}$$

For the obtained two areas, the same procedure as described above is conducted. The model stops splitting nodes when the mean squared error per node drops below the the threshold, the default threshold is 1e-6. Finally, we obtain a tree that divides the space into N areas $R_1, R_2, R_3, ...R_N$.

In this paper, we focus on pedestrian flow model development; therefore, we use the MATLAB software, which has a machine learning and deep learning toolbox, to build the linear regression, neural network and decision tree models [41]. The default parameters are selected so that we can compare the model performance under the same condition.

4) PREDICTION MODEL SELECTION CRITERIA

The errors of the prediction model can be defined as:

$$e_k = \alpha_k - \widehat{\alpha_k} \tag{12}$$

where α_k and $\widehat{\alpha_k}$ are the true value and predicted value of walking direction, respectively. The mean absolute error (MAE), root mean square error (RMSE) and R squared are used as performance measures in our model comparison. The three indicators are defined as follows:

$$MAE = \frac{1}{K} \sum_{k=1}^{K} |e_m| \tag{13}$$

$$RMSE = \sqrt{\frac{1}{K} \sum_{k=1}^{K} (e_k)^2} \tag{14}$$

$$R^2 = 1 - \frac{\sum_{k=1}^{K} (e_k)^2}{\sum_{k=1}^{K} (\alpha_k - \overline{\alpha})^2} \tag{15}$$

where K is the number of observations and $\overline{\alpha}$ is the average value of the walking direction.

Because the three indicators only present the prediction performance, however, the direction decision model (DDM) is incorporated into the simulation model; therefore, the model capability to describe the pedestrian flow behavior should be compared to select the best DDM. In our experiment, the individual trajectory and the collective pattern of different models are presented in a simulated environment.

IV. ACCELERATION AND BODY COLLISION MODEL

After predicting the value of α, the desired walking direction $\overrightarrow{\kappa} = (sin(\alpha), -cos(\alpha))$. However, the desired walking direction of all pedestrians is produced using the same prediction model, which cannot reflect the crowd heterogeneity. To solve this problem, we add random noise to the desired walking direction in order to describe the variety of direction choice.

The random noise ξ is produced from the normal distribution $N(\sigma, \mu)$. σ and μ are equal to the standard derivation and the average value of the errors of the prediction model $e_m, m = 1, 2, 3...M$. Therefore, the desired walking direction of pedestrian i is defined as:

$$\overrightarrow{\kappa}_i = (sin(\alpha_i + \xi_i), -cos(\alpha_i + \xi_i)), \xi_i \sim N(\sigma, \mu) \quad (16)$$

The pedestrians accelerate and walk at their desired speed. The acceleration is defined as:

$$\frac{d\overrightarrow{v_i}}{dt} = \frac{(v_i^f \overrightarrow{\kappa}_i - \overrightarrow{v_i})}{\tau} \quad (17)$$

where τ is the pedestrian relaxation time, $\overrightarrow{v_i}$ is the walking speed of pedestrian i and $\overrightarrow{v_i^f}$ is the desired walking speed of pedestrian i. Assume that the body of a pedestrian is a circle. Let r_i denote the radius of pedestrian i. To avoid collisions with neighboring pedestrians and walls, the repulsive force from neighboring pedestrians can be defined as follows:

$$f_{ij} = \omega g(r_{ij} - d_{ij})\vec{n}_{ij} \quad (18)$$

where $r_{ij} = r_i + r_j$, d_{ij} is the distance between pedestrian i and j. If the pedestrians touch each other, $r_{ij} - d_{ij} > 0$, then $g(x) = x$, otherwise, $g(x) = 0$. $\vec{n}_{ij}$ is the normalized vector pointing from pedestrian j to i. Similarly, the repulsive force from neighboring walls can be defined as:

$$f_{iw} = \omega g(r_i - d_{iw})\vec{n}_{iw} \quad (19)$$

where d_{iw} is the distance between pedestrian i and wall w. $\vec{n}_{iw}$ is the normalized vector pointing from wall w to pedestrian i. In summary, the pedestrian can be regarded as an agent who is driven by the force

$$\frac{d\overrightarrow{v_i}}{dt} = \frac{(v_i^f \overrightarrow{e} - \overrightarrow{v_i})}{\tau} + \frac{\sum f_{ij}}{m_i} + \frac{\sum f_{iw}}{m_i} \quad (20)$$

where m_i is the mass of pedestrian i. Therefore, the location of pedestrian i can be updated as follows:

$$\frac{d\overrightarrow{p_i}}{dt} = \overrightarrow{v_i} \quad (21)$$

Because the model is proposed by integrating the three prediction models and the social force model, we can obtain three pedestrian flow models named LR-SFM, NN-SFM and DT-SFM.

V. RESULTS

A. DATA DESCRIPTION

The data used in this paper comes from the bidirectional pedestrian flow experiment [42]. The pedestrian trajectories are recorded using PeTrack software and a marker-based tracking algorithm [43]. Fig.4 shows the snapshot and the corresponding trajectories. The features are extracted from the trajectories and 166725 samples are obtained finally.

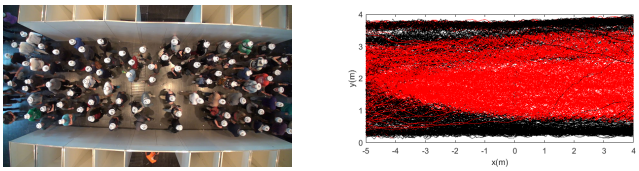

(a) snapshot (b) Pedestrian trajectories

FIGURE 4. Snapshot and pedestrian trajectories.

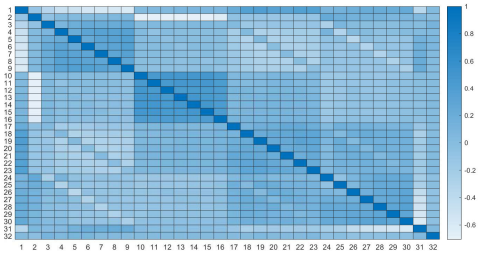

FIGURE 5. Correlation coefficient of each two different features.

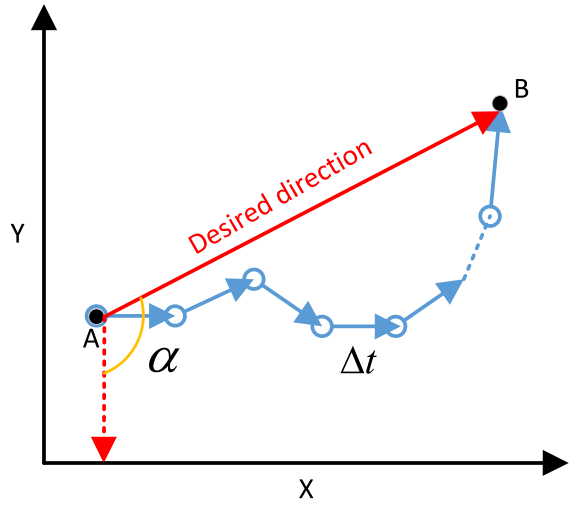

FIGURE 6. Desired direction calculation.

B. PREDICTION PERFORMANCE COMPARISON

The correlation of the selected features is depicted in Fig.5. We found that the correlation coefficient of each of the two different features ranges from -0.71 to 0.4926. Therefore, we believe that the 32 selected features are independent and thus can be used to predict the desired walking direction.

The time interval for collecting data in the experiment is 0.0625 s, which is so small that the desired walking direction decision cannot be reflected. Furthermore, the walking direction in real life will change if a body collision occurs; therefore, we adopt a larger time interval to reduce the effect of collisions on the desired walking direction, and then the desired walking direction can be obtained as indicated by Fig.6. The time interval is set to 30 times of 0.0625 s (1.875 s) s in our experiment because

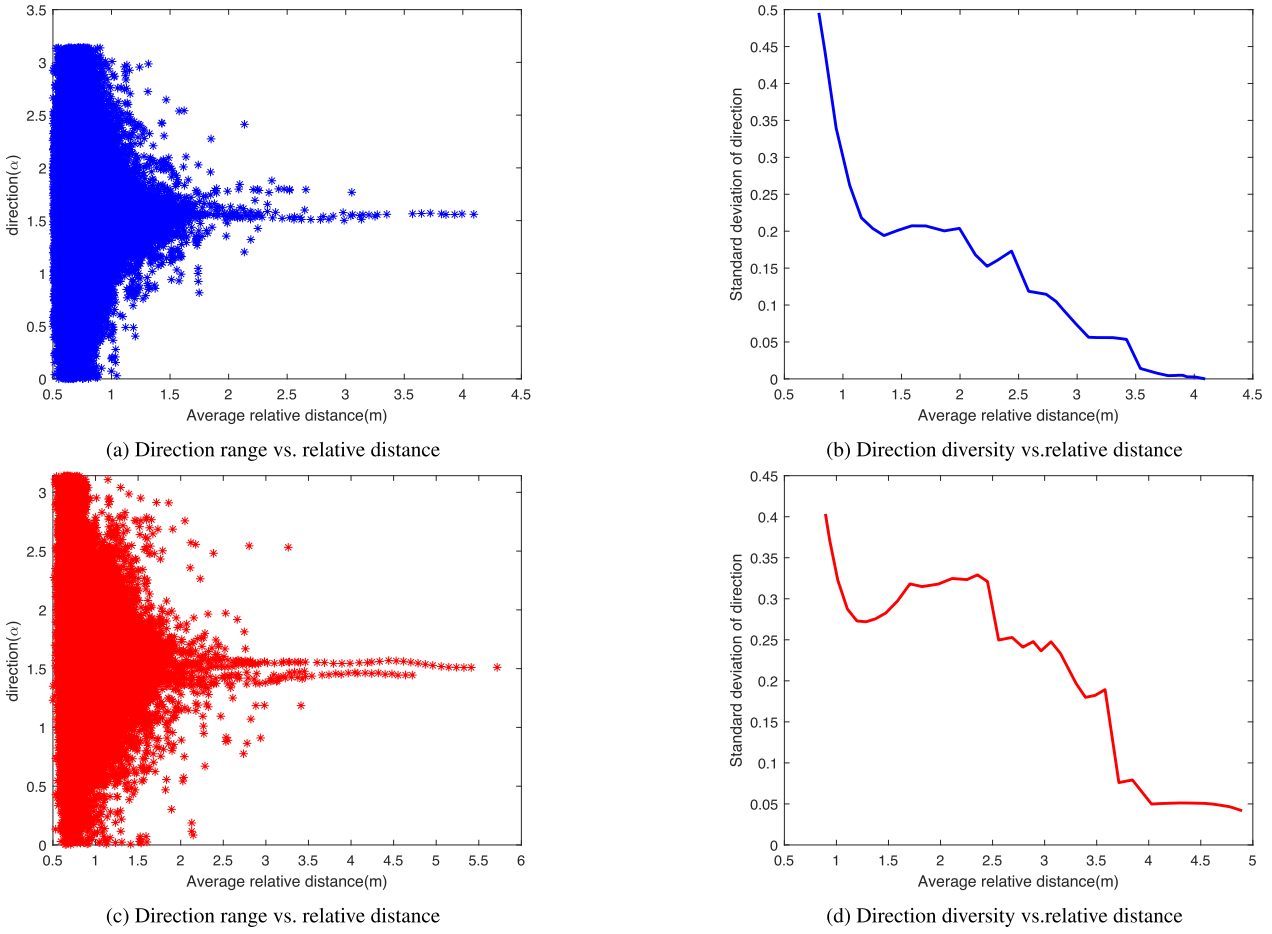

(a) Direction range vs. relative distance

(b) Direction diversity vs.relative distance

(c) Direction range vs. relative distance

(d) Direction diversity vs.relative distance

FIGURE 7. The relationship between direction decision and relative distance, (a)(b)left-going pedestrians, (c)(d)right-going pedestrians.

the performance of the three models is acceptable in this case.

Fig.7 shows the relationship between direction decision and relative distance. Fig.7a and Fig.7b show the relationship between direction decision and relative distance derived from the trajectories of left-going pedestrians. Fig.7c and Fig.7d show the relationship between direction decision and relative distance derived from the trajectories of right-going pedestrians. The standard deviation is used to denote the direction diversity as shown in Fig.7b and Fig.7d. If the relative distance is shorter, the pedestrian prefers to change his/her walking direction in a larger range as shown in Fig.7a and Fig.7c. As a result, the standard deviation of direction choice of left-going pedestrians decreases from 0.50 to 0 as the relative distance increases from 0.5 m to 4 m, the standard deviation of direction choice of right-going pedestrians decreases from 0.40 to 0.04 as the relative distance increases from 0.90 m to 4.90 m.

The longer relative distance means less congestion in the pedestrians' vision, therefore the pedestrians can walk with a free walking speed and thus have no need to adjust their direction if the relative distance is long enough. The results show that the relative distance can affect the direction decision behavior of pedestrians and the relative distance features should be used to determine the desired walking direction.

Fig.8 shows the relationship between direction decision and relative speed. Fig.8a and Fig.8b show the relationship between direction decision and relative speed derived from the trajectories of left-going pedestrians. Fig.8c and Fig.8d show the relationship between direction decision and relative speed derived from the trajectories of right-going pedestrians. The standard deviation is used to denote the direction diversity as shown in Fig.8b and Fig.8d. If the relative speed is smaller, the pedestrian prefers to change his/her walking direction in a larger range as shown in Fig.8a and Fig.8c. As a result, the standard deviation of direction choice of left-going pedestrians decreases from 0.50 to 0.027 as the relative speed increases from 0.259 m/s to 1.6 m/s, the standard deviation of direction choice of right-going pedestrians decreases from 0.40 to 0.05 as the relative distance increases from 0.29 m/s to 1.6 m/s. The longer relative distance means less congestion in the pedestrians' vision, therefore the pedestrians can walk with a free walking speed and thus have no need to adjust

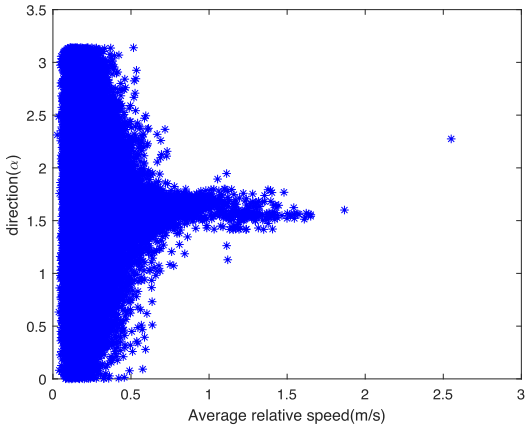

(a) Direction range vs. relative speed

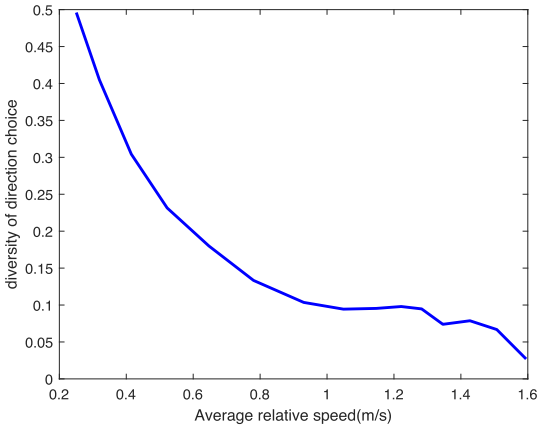

(b) Direction diversity vs.relative speed

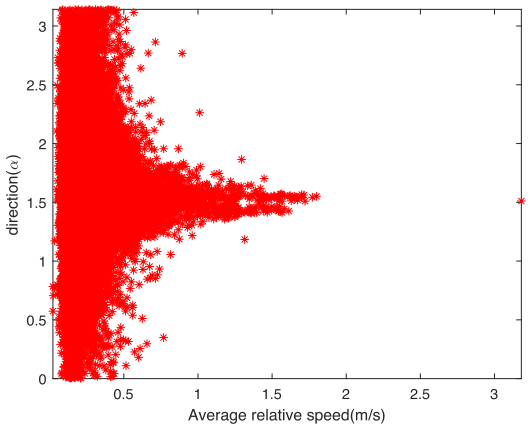

(c) Direction range vs. relative speed

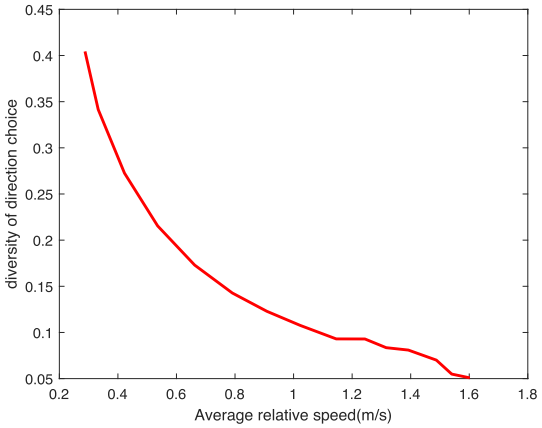

(d) Direction diversity vs.relative speed

FIGURE 8. The relationship between direction decision and relative speed, (a)(b)left-going pedestrians, (c)(d)right-going pedestrians.

TABLE 1. Prediction performance of the DDM.

Prediction performance	MAE	RMSE	R^2
LR	0.1266	0.1838	0.0267
NN	0.1089	0.1539	0.3172
DT	0.0227	0.0414	0.9505

their direction if the relative distance is long enough. The results show that the relative speed can affect the direction decision behavior of pedestrians and the relative speed features should be used to determine the desired walking direction.

The performance of the three prediction models is compared when the vision field of pedestrians $\theta = \pi$. Table.1 lists the MAE, RMSE and R squared of the three prediction models. As seen in Table.1, the DT model performs much better than the other two models because it has the lowest MAE, the lowest RMSE and the highest R squared. Therefore, the DT model is the best model for predicting the desired walking direction of pedestrians.

The effect of the number of neighboring pedestrians on the RMSE is depicted in Fig.9. As described in section III-A,

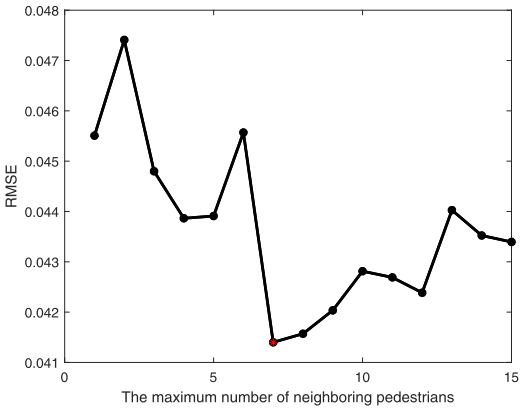

FIGURE 9. Effect of number of neighboring pedestrians on the RMSE.

more neighboring pedestrians produce more features. however, the DT model has the best prediction performance when the number of neighboring pedestrians is equal to 7. The result shows that the pedestrians make direction decision based on the state of 7 neighboring pedestrians at most. Therefore, 7 neighboring pedestrians are selected

TABLE 2. The number of corresponding features.

No.	1	2	3-9	10-16
Feature	v_i^x	v_i^y	$v_i^x - v_j^x$	$v_i^y - v_j^y$
No.	17-23	24-30	31	32
Feature	$x_i - x_j$	$y_i - y_j$	y_i/W	$L - x_i$

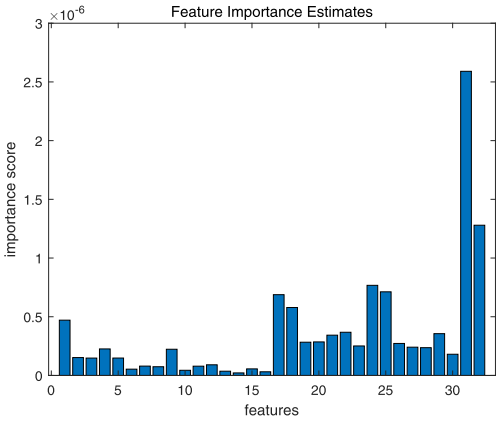

FIGURE 10. Feature importance measure.

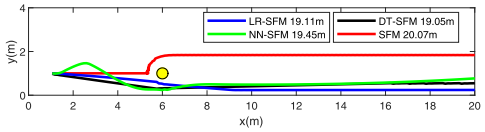

FIGURE 11. Trajectories recorded in the simulation.

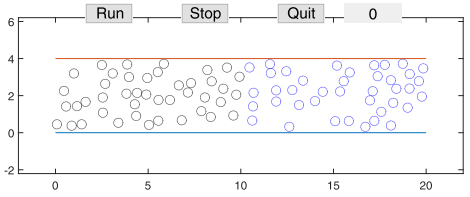

FIGURE 12. The initial state of the bidirectional corridor.

to produce the features to efficiently predict the walking direction.

We did't present the tree graph because the decision tree has 2653 nodes (1327 leaf nodes and 1326 branch nodes). We estimate importance values of features by summing changes in the risk due to splits on every feature and dividing the sum by the number of branch nodes. A bar graph is depicted in Fig.10 to compare the estimates. The number and the corresponding features in Fig.10 is listed in Table.2. The top two features influencing the desired walking direction prediction are the distance to the target and wall because the pedestrians want to walk to the destination in the physical space restricted by the walls. The relative distance to the neighboring pedestrians are also considered as important features in the DT model. It can be found that the importance of relative distance to the nearer neighbors is much more than the counterpart to the farther neighbors which accords with the perceptual characteristics of pedestrians. We also found that the relative speed features have the least importance. The fact reveals that the pedestrians prefer to make direction decision based on the relative distance because the pedestrians can sense the relative distance features much more easily than the relative speed features.

C. MODEL PERFORMANCE COMPARISON

The prediction models are also evaluated by predicting the desired walking direction in a simulation environment. The performances of different models, including the proposed model with different prediction models (LR-SFM, NN-SFM, DT-SFM) and the original social force model, are compared. The parameters are defined as follows: the time step of the simulation model is 0.0625 s, the desired walking speed $v_i^f = 1.1\ m/s$ based on the experimental data and the relaxation time $\tau = 0.5\ s$ in Eq.17, the pedestrian radius $r_i = 0.25m$ and $\omega = 2000\ N$ in Eq.18 and 19.

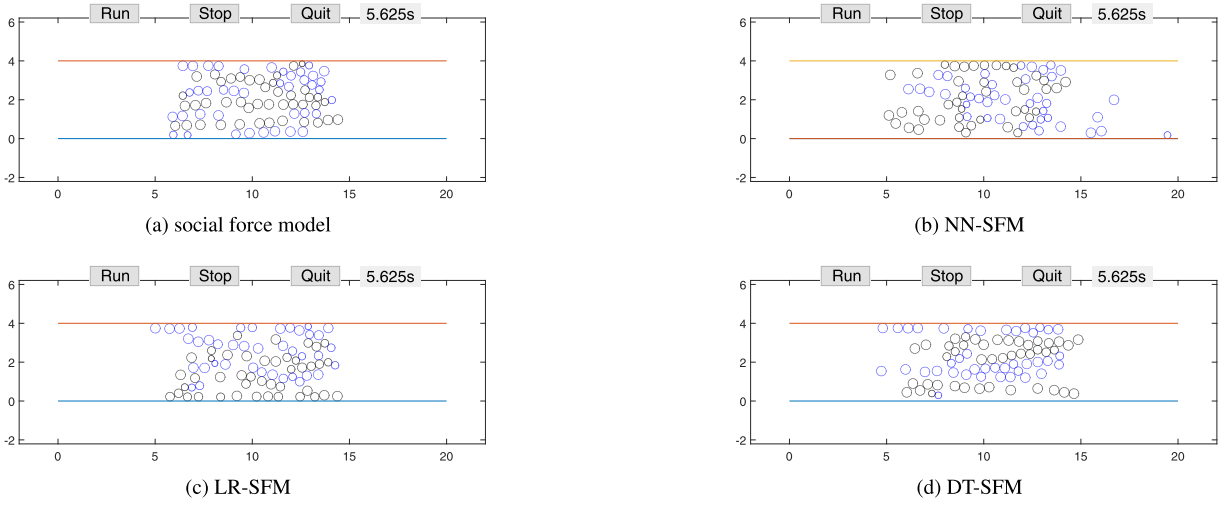

(a) social force model (b) NN-SFM

(c) LR-SFM (d) DT-SFM

FIGURE 13. The traffic state of the corridor at time=5.625 s.

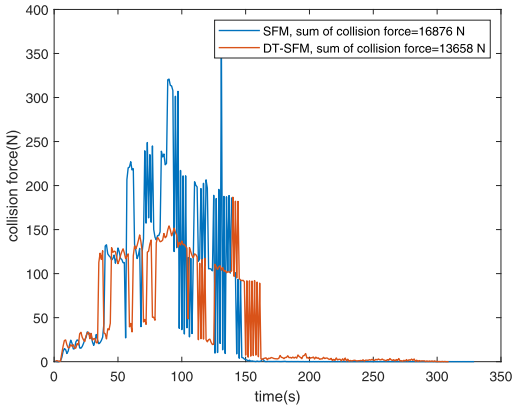

FIGURE 14. Collision force in SFM and DT-SFM.

1) INDIVIDUAL TRAJECTORIES

First, we tested the model in the context of simple interaction situations involving two pedestrians avoiding each other. One pedestrian passed the other pedestrian standing in the corridor with a width of 3 m and a length of 20 m. The trajectories resulting from the DT-SFM, SFM and LR-SFM were recorded in Fig.11. The pedestrian in SFM changed his/her direction only when he/she encountered standing pedestrians; however, the pedestrian in DT-SFM, LR-SFM and NN-SFM selected the direction in which the collision could be avoided in advance. As shown in Fig.11, the length of the trajectory produced by the SFM, NN-SFM, LR-SFM and DT-SFM is 20.07 m, 19.45 m, 19.11 m and 19.05 m; therefore, the DT-SFM produced the shortest path for the pedestrians. Furthermore, the LR-SFM produced the desired walking direction, which caused the moving pedestrian to hit the wall after the moving pedestrian passed the standing pedestrian.

2) COLLECTIVE PATTERN OF MOTION

We compared the performance of the proposed model in the simulation of bidirectional pedestrian flow. The initial state is depicted in Fig.12. The length and width of the bidirectional corridor were 20 m and 4 m, respectively. There were 43 pedestrians walking to the right end of the corridor and 40 pedestrians walking to the left end of the corridor.

The pedestrian traffic state of the corridor at time=5.625 s is depicted in Fig.13. Fig.13a shows the pedestrian traffic state of the SFM model; Lane formation is one typical phenomenon in pedestrian counter flow, however, the lanes are not formed clearly in the bidirectional pedestrian flow because the pedestrians in the SFM cannot change their desired walking direction based on the neighboring environment. Fig.13b shows the pedestrian traffic state of the NN-SFM model; some pedestrians in the NN-SFM cannot realize their destination clearly, and the lane formation phenomenon also was not found in the bidirectional pedestrian flow because the NN-SFM had poor prediction performance. The pedestrian traffic state of the LR-SFM model shows that pedestrians could walk to their destination; however, the lane formation phenomenon was not found in Fig.13c due to the poor prediction performance of the linear regression model. The pedestrian traffic state of the DT-SFM model shows that pedestrians could walk to their destination, and the clear lane formation phenomenon was shown in Fig.13d because the decision tree model had the best prediction performance.

The collision force (Eq.18 and 19) experienced by pedestrians in SFM and DT-SFM is depicted in Fig.14. As shown in Fig.14, the collision force of SFM and DT-SFM increased largely when the two pedestrian streams met; however, the collision force of DT-SFM increased much less than the SFM. The sum of the collision force of SFM was 16876 N, while the sum of the collision force of DT-SFM was 13658 N. Therefore, the proposed direction decision model reduced the collision level largely, which meets the expectation of pedestrians. The results show that pedestrians tend to walk in uncongested conditions.

Fig.15 compared the simulation performance of our model and the artificial intelligence model proposed by [16]. It can be seen that some pedestrians in Fig.15a overlap with neighboring pedestrians, and some pedestrians hit the wall; therefore, the collision avoidance problem cannot be solved if only the data-driven velocity prediction model is used. We believe that the collision avoidance problem can be solved if enough data are used to train the AIM; however, it will require considerable time and money to collect data. No conflicts in Fig.15b occur because the collision avoidance model is applied; therefore, our model solved the collision avoidance problem.

(a) AIM (b) DT-SFM

FIGURE 15. The traffic state of the corridor at time=5.625 s.

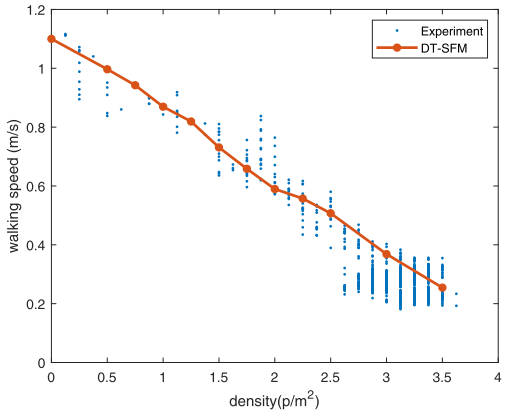

FIGURE 16. Fundamental diagram comparison.

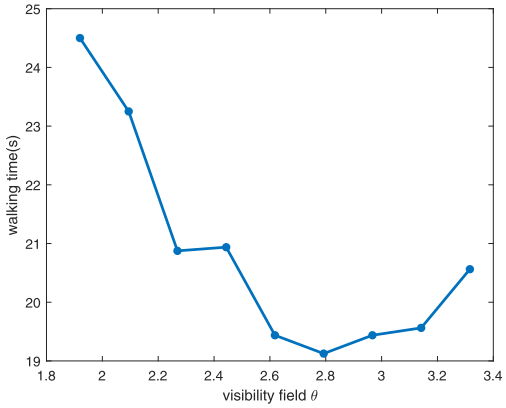

FIGURE 17. Effect of visibility field on the walking time.

The speed-density relationship resulting from the DT-SFM and experiment is shown in Fig.16. The R squared is 0.998 and the root mean squared error is 0.0099, therefore, the obtained fundamental diagram fit well with the experimental data. The speed is a linear decreasing function with respect to density.

D. SENSITIVITY ANALYSIS

In the proposed model, it is difficult to determine the visibility field and the desire to change direction, therefore, the effect of visibility field and the desire to change direction on the pedestrian flow is investigated in this section.

1) VISIBILITY FIELD (θ)

Fig.17 depicts the relationship between the visibility field and walking time. The walking time decreased from 24.5s to 19.13s as the visibility field of pedestrians increased from 1.92 to 2.8, and then the walking time increased from 19.13s to 20.56s as the visibility field of pedestrians increased from 2.8 to 3.316. Therefore, there is an optimal visibility field to realize the highest traffic efficiency. The results show that the traffic efficiency can be improved by considering the effect of neighboring pedestrians in a larger visibility range when the visibility field $\theta < 2.8$, however, when the visibility field $\theta \geq 2.8$, the traffic efficiency can not be improved although a larger visibility range is adopted.

2) DIRECTION CHANGING FREQUENCY

We defined the time interval of desired walking direction as the time from the start to the end of desired walking direction α. The time interval of the desired walking direction reflects the direction changing frequency and is determined by the neighborhood environment. For example, if the time interval of the desired walking direction is 0.5 s, the pedestrians change their direction 2 times every 1 second. Therefore, we analyzed the effect of direction changing frequency on pedestrian flow. Fig.18 depicts the pedestrians' trajectory when the time interval of direction changing was equal to 0.0625 s, 0.625 s, 1.25 s, and 1.875 s. It can be seen that pedestrians with higher direction changing frequency avoided conflicts from the counterflow in a timely manner; thus, fewer trajectories intersected in Fig.18c and 18d and thus the corresponding collision forces are lower (13658 N, 14532 N); however, the pedestrians with low direction changing frequency could not avoid conflicts from the counterflow, and more trajectories intersected in Fig.18a and 18b and thus the corresponding collision forces are larger (17722 N, 23319 N).

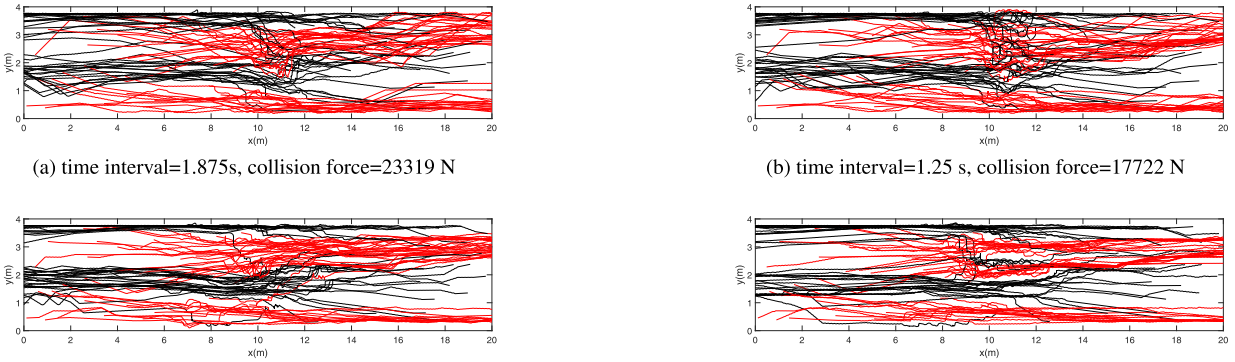

(a) time interval=1.875s, collision force=23319 N

(b) time interval=1.25 s, collision force=17722 N

(c) time interval=0.625 s, collision force=14532 N

(d) time interval=0.0625 s, collision force=13658 N

FIGURE 18. The trajectories of pedestrians and collision force under various direction changing frequencies.

VI. CONCLUSION AND EXTENSION

We proposed a microscopic simulation model of pedestrian flow by combining the direction decision and social force model. First, the trajectory of pedestrians from video was collected to train the prediction models, and the model with the best performance was used to predict the desired walking direction of pedestrians in simulation. Second, the acceleration and collision avoidance model was proposed to simulate the crowd movement in corridors. Finally, an experiment was conducted to prove the efficiency of the model.

The feature importance, which reflects the effect of each feature on the desired direction, was measured. The corridor geometry was the most important factor influencing the desired walking direction, and the relative distance features were much more important than the relative velocity features. The relative distance features to the nearer pedestrian were more important than the counterpart to farther pedestrians.

The proposed model can be used to simulate the pedestrian counterflow in corridors with various widths and lengths. The DT-SFM performs better in simulating the individual trajectory and lane formation of bidirectional pedestrian flow than the other models. Compared to the AIM, which uses only the machine learning-based prediction model, the proposed DT-SFM can simulate the collision avoidance behavior of pedestrians. Compared to the SFM, collisions can be largely reduced by the DDM. The speed-density relationship from the simulation model fits the experimental data well.

The sensitivity analysis shows that there is an optimal visibility field to realize the highest traffic efficiency. The direction changing frequency has effects on the lane formation of bidirectional pedestrian flow. The simulation results show that pedestrians with high direction changing frequency prefer to avoid conflicts from the counterflow and that pedestrians with similar directions prefer to flock together. However, there are more trajectory conflicts if the pedestrians do not change their desired walking direction frequently according to the dynamic neighboring environment. In the future, the trajectory data of pedestrians in corridors with various geometries can also be used to train the desired walking direction model, and the desired walking direction model will be combined with other microscopic pedestrian flow models, such as the cellular automata model, to simulate the pedestrian flow.

REFERENCES

[1] H. Guo, W. Wang, W. Guo, X. Jiang, and H. Bubb, "Reliability analysis of pedestrian safety crossing in urban traffic environment," *Saf. Sci.*, vol. 50, no. 4, pp. 968–973, Apr. 2012.

[2] H. Vermuyten, J. Beliën, L. De Boeck, G. Reniers, and T. Wauters, "A review of optimisation models for pedestrian evacuation and design problems," *Saf. Sci.*, vol. 87, pp. 167–178, Aug. 2016.

[3] W. Zeng, P. Chen, H. Nakamura, and M. Iryo-Asano, "Application of social force model to pedestrian behavior analysis at signalized crosswalk," *Transp. Res. C, Emerg. Technol.*, vol. 40, pp. 143–159, Mar. 2014.

[4] H.-Y. Shang, H.-J. Huang, and Y.-M. Zhang, "An extended mobile lattice gas model allowing pedestrian step size variable," *Phys. A, Stat. Mech. Appl.*, vol. 424, pp. 283–293, Apr. 2015.

[5] Z.-J. Ding, Y.-H. Huang, T. Liu, J.-X. Ding, W. Hu, R. Jiang, and B.-H. Wang, "Analytical and simulation studies of intersecting pedestrian flow on the 2D lattice with parallel update rule," *Phys. A, Stat. Mech. Appl.*, vol. 523, pp. 1183–1201, Jun. 2019.

[6] D. Li and B. Han, "Behavioral effect on pedestrian evacuation simulation using cellular automata," *Saf. Sci.*, vol. 80, pp. 41–55, Dec. 2015.

[7] L. Crociani and G. Lämmel, "Multidestination pedestrian flows in equilibrium: A cellular automaton-based approach," *Comput.-Aided Civil Infrastruct. Eng.*, vol. 31, no. 6, pp. 432–448, Jun. 2016.

[8] J. Hu, L. You, H. Zhang, J. Wei, and Y. Guo, "Study on queueing behavior in pedestrian evacuation by extended cellular automata model," *Phys. A, Stat. Mech. Appl.*, vol. 489, pp. 112–127, Jan. 2018.

[9] Y. Li, D. Z. W. Wang, M. Meng, and K. Wang, "Simulation of pedestrian evacuation in university canteen based on cellular automata," *IEEE Access*, vol. 7, pp. 130120–130132, 2019.

[10] L. Chen, T.-Q. Tang, H.-J. Huang, J.-J. Wu, and Z. Song, "Modeling pedestrian flow accounting for collision avoidance during evacuation," *Simul. Model. Pract. Theory*, vol. 82, pp. 1–11, Mar. 2018.

[11] Q.-Y. Hao, R. Jiang, M.-B. Hu, and Q.-S. Wu, "Unidirectional pedestrian flow in a lattice gas model coupled with game theory," in *Proc. 4th Int. Joint Conf. Comput. Sci. Optim.*, Apr. 2011, pp. 1054–1058.

[12] W. Weng, T. Chen, H. Yuan, and W. Fan, "Cellular automaton simulation of pedestrian counter flow with different walk velocities," *Phys. Rev. E, Stat. Phys. Plasmas Fluids Relat. Interdiscip. Top.*, vol. 74, no. 3, 2006, Art. no. 036102.

[13] L. Luo, Z. Fu, H. Cheng, and L. Yang, "Update schemes of multi-velocity floor field cellular automaton for pedestrian dynamics," *Phys. A, Stat. Mech. Appl.*, vol. 491, pp. 946–963, Feb. 2018.

[14] Y. Li, M. Chen, Z. Dou, X. Zheng, Y. Cheng, and A. Mebarki, "A review of cellular automata models for crowd evacuation," *Phys. A, Stat. Mech. Appl.*, vol. 526, Jul. 2019, Art. no. 120752.

[15] S. Kim, S. J. Guy, W. Liu, D. Wilkie, R. W. Lau, M. C. Lin, and D. Manocha, "BRVO: Predicting pedestrian trajectories using velocity-space reasoning," *Int. J. Robot. Res.*, vol. 34, no. 2, pp. 201–217, Feb. 2015.

[16] X. Song, D. Han, J. Sun, and Z. Zhang, "A data-driven neural network approach to simulate pedestrian movement," *Phys. A, Stat. Mech. Appl.*, vol. 509, pp. 827–844, Nov. 2018.

[17] Q. Xu, M. Chraibi, A. Tordeux, and J. Zhang, "Generalized collision-free velocity model for pedestrian dynamics," *Phys. A, Stat. Mech. Appl.*, vol. 535, Dec. 2019, Art. no. 122521.

[18] D. Helbing, I. Farkas, and T. Vicsek, "Simulating dynamical features of escape panic," *Nature*, vol. 407, no. 6803, pp. 487–490, Sep. 2000.

[19] Z. Yuan, R. Guo, S. Tang, B. He, L. Bian, and Y. Li, "Simulation of the separating crowd behavior in a T-shaped channel based on the social force model," *IEEE Access*, vol. 7, pp. 13668–13682, 2019.

[20] X. Chen, M. Treiber, V. Kanagaraj, and H. Li, "Social force models for pedestrian traffic—State of the art," *Transp. Rev.*, vol. 38, no. 5, pp. 625–653, Sep. 2018.

[21] M. Chraibi, U. Kemloh, A. Schadschneider, and A. Seyfried, "Force-based models of pedestrian dynamics," *Netw. Heterogeneous Media*, vol. 6, no. 3, pp. 425–442, 2011.

[22] A. Johansson, D. Helbing, and P. K. Shukla, "Specification of the social force pedestrian model by evolutionary adjustment to video tracking data," *Adv. Complex Syst.*, vol. 10, pp. 271–288, Dec. 2007.

[23] M. Li, Y. Zhao, L. He, W. Chen, and X. Xu, "The parameter calibration and optimization of social force model for the real-life 2013 ya'an earthquake evacuation in China," *Saf. Sci.*, vol. 79, pp. 243–253, Nov. 2015.

[24] J. Song, F. Chen, Y. Zhu, N. Zhang, W. Liu, and K. Du, "Experiment calibrated simulation modeling of crowding forces in high density crowd," *IEEE Access*, vol. 7, pp. 100162–100173, 2019.

[25] M. Asano, A. Sumalee, M. Kuwahara, and S. Tanaka, "Dynamic cell transmission–based pedestrian model with multidirectional flows and strategic route choices," *Transp. Res. Rec.*, vol. 2039, no. 1, pp. 42–49, Jan. 2007.

[26] F. S. Hänseler, M. Bierlaire, B. Farooq, and T. Mühlematter, "A macroscopic loading model for time-varying pedestrian flows in public walking areas," *Transp. Res. B, Methodol.*, vol. 69, pp. 60–80, Nov. 2014.

[27] S. Liu, S. Lo, J. Ma, and W. Wang, "An agent-based microscopic pedestrian flow simulation model for pedestrian traffic problems," *IEEE Trans. Intell. Transp. Syst.*, vol. 15, no. 3, pp. 992–1001, Jun. 2014.

[28] M. Moussaid, D. Helbing, and G. Theraulaz, "How simple rules determine pedestrian behavior and crowd disasters," *Proc. Nat. Acad. Sci. USA*, vol. 108, no. 17, pp. 6884–6888, Apr. 2011.

[29] X. Yao, Y. Lian, and C. Wei, "A Markov jump approach to modeling and analysis of pedestrian dynamics," *IEEE Access*, vol. 7, pp. 87808–87815, 2019.
[30] F. Martinez-Gil, M. Lozano, and F. Fernández, "MARL-Ped: A multi-agent reinforcement learning based framework to simulate pedestrian groups," *Simul. Model. Pract. Theory*, vol. 47, pp. 259–275, Sep. 2014.
[31] Y. Ma, E. W. M. Lee, and R. K. K. Yuen, "An artificial intelligence-based approach for simulating pedestrian movement," *IEEE Trans. Intell. Transp. Syst.*, vol. 17, no. 11, pp. 3159–3170, Nov. 2016.
[32] A. Alahi, K. Goel, V. Ramanathan, A. Robicquet, L. Fei-Fei, and S. Savarese, "Social LSTM: Human trajectory prediction in crowded spaces," in *Proc. IEEE Conf. Comput. Vis. Pattern Recognit. (CVPR)*, Jun. 2016, pp. 961–971.
[33] H. Xue, D. Q. Huynh, and M. Reynolds, "SS-LSTM: A hierarchical LSTM model for pedestrian trajectory prediction," in *Proc. IEEE Winter Conf. Appl. Comput. Vis. (WACV)*, Mar. 2018, pp. 1186–1194.
[34] A. Miguel, "Constructal theory of pedestrian dynamics," *Phys. Lett. A*, vol. 373, no. 20, pp. 1734–1738, Apr. 2009.
[35] M. Razi and K. Athappilly, "A comparative predictive analysis of neural networks (NNs), nonlinear regression and classification and regression tree (CART) models," *Expert Syst. Appl.*, vol. 29, no. 1, pp. 65–74, Jul. 2005.
[36] G. K. Tso and K. K. Yau, "Predicting electricity energy consumption: A comparison of regression analysis, decision tree and neural networks," *Energy*, vol. 32, no. 9, pp. 1761–1768, Sep. 2007.
[37] M. Frederick, "Neuroshell 2 manual," Ward Syst. Group, Frederick, MD, USA, Tech. Rep., 1996, vol. 2.
[38] P. Kim, "MATLAB deep learning," in *With Machine Learning, Neural Networks and Artificial Intelligence*, vol. 130. New York, NY, USA: Springer, 2017.
[39] J. R. Quinlan, *C4. 5: Programs for Machine Learning*. Amsterdam, The Netherlands: Elsevier, 2014.
[40] W.-Y. Loh, "Classification and regression tree methods," in *Wiley StatsRef: Statistics Reference Online*. Hoboken, NJ, USA: Wiley, 2014.
[41] M. Levy, D. Raviv, and J. Baker, "Data center predictions using MATLAB machine learning toolbox," in *Proc. IEEE 9th Annu. Comput. Commun. Workshop Conf. (CCWC)*, Jan. 2019, pp. 0458–0464.
[42] J. Zhang, W. Klingsch, A. Schadschneider, and A. Seyfried, "Ordering in bidirectional pedestrian flows and its influence on the fundamental diagram," *J. Stat. Mech.*, vol. 2012, no. 2, Feb. 2012, Art. no. P02002.
[43] Y. Malinovskiy, J. Zheng, and Y. Wang, "A simple and model-free algorithm for real-time pedestrian detection and tracking," in *Proc. 86th Annu. Meeting Transp. Res. Board*, Washington, DC, USA, 2007.

ZHE ZHANG was born in 1988. He received the Ph.D. degree in transportation engineering from Beijing Jiaotong University, in 2017. He is currently a Researcher with the State Key Laboratory of Rail Traffic Control, Beijing Jiaotong University. His research interests include pedestrian flow simulation, crowd control, and facility optimization in terminals.

LIMIN JIA received the Ph.D. degree in automation and control in transportation from the China Academy of Railway Sciences, Beijing, China, in 1991. He is currently a Professor with Beijing Jiaotong University, and the Chief Scientist of the National Center of Collaborative Innovation Center for Rail Safety and the State Key Laboratory of Rail Traffic Control and Safety. His research interests include intelligent transportation systems, computational intelligence, and rail traffic control and safety.